Measuring Induction Period for Calcium Sulfate Dihydrate Precipitation

Amedeo Lancia
Dip. di Ingegneria Chimica, Università di Napoli "Federico II," P. le Tecchio 80, 80125 Napoli, Italy

Dino Musmarra
Istituto di Ricerche sulla Combustione, CNR, P. le Tecchio 80, 80125 Napoli, Italy

Marina Prisciandaro
Dip. di Chimica, Ingegneria Chimica e Materiali, Università di L'Aquila, Monteluco di Roio, 67040 L'Aquila, Italy

Homogeneous nucleation of $CaSO_4 \cdot 2H_2O$ (gypsum) based on an optical diagnostic technique was studied within a supersaturation range of 1–4 at 25–90°C. The experiments were carried out using an experimental apparatus consisting of a batch crystallizer with the related measurement devices. Signals of scattered and transmitted light coming from a He–Ne laser source were analyzed to measure the induction period (t_{ind}), that is, the time delay necessary for homogeneous nucleation to take place. As expected from theory, it was found that t_{ind} decreases when either temperature or supersaturation increase; from the dependence of t_{ind} on supersaturation, it was possible to distinguish between the mechanisms of homogeneous and heterogeneous nucleation. From the experimental data relative to homogeneous nucleation, the interfacial tension (γ_s) between $CaSO_4 \cdot 2H_2O$ and the surrounding aqueous solution and the activation energy (E_{att}) for $CaSO_4 \cdot 2H_2O$ crystallization were evaluated. In particular, the dependence of t_{ind} on temperature made it possible to evaluate E_{att} at 30 kJ/mol and the dependence of t_{ind} on supersaturation offered the value of γ_s to be about 37 mJ/m^2, which does not vary with temperature in the interval explored.

Introduction

The wet limestone-gypsum flue-gas desulfurization process is the most widely used method to reduce sulfur dioxide emissions into the atmosphere by combustion of fossil fuels. In this process SO_2 is absorbed by a limestone suspension in a multistage turbulent absorber or a spray tower. Downstream from the absorber, a hold tank in which air is sparged is provided: in the tank oxidation of calcium sulfite takes place, together with the crystallization of a solid byproduct mostly made of gypsum ($CaSO_4 \cdot 2H_2O$). The crystal habit of the gypsum produced is an important aspect of wet limestone scrubbing, since it significantly affects the byproduct dewatering properties, and consequently the economics of the whole process.

A significant amount of work has been done to improve the understanding of the nucleation and growth mechanisms of $CaSO_4 \cdot 2H_2O$ crystals, both with a fundamental and an operating approach. For what concerns crystal nucleation kinetics, an important parameter is the time which elapses between the onset of supersaturation and the formation of critical nuclei, or *embryos* (clusters of loosely aggregated molecules which have the same probability of growing to become crystals or dissolving to disappear into the mother solution). This time, defined as *true induction period* (t^*) (s), primarily depends on solution supersaturation and temperature. However, as pointed out by Söhnel and Mullin (1978), t^* cannot be experimentally measured, since it is not possible to detect the formation of critical nuclei; rather, in order to perform the measurements, it is necessary to let such nuclei grow until they reach a detectable size. Consequently, it is possible to experimentally evaluate only a time referred to simply as

Correspondence concerning this article should be addressed to A. Lancia.

induction period (t_{ind}) (s), with $t_{ind} \geq t^*$, defined as the time elapsed between the onset of supersaturation and the first changes in the system physical properties due to the formation of a solid phase (Söhnel and Garside, 1992). It has to be observed that t_{ind} cannot be considered a fundamental property of the system, since its value depends on the technique employed to detect the formation of the solid phase; nevertheless an analysis of experimentally determined values of t_{ind} can give some important information about the mechanisms of solid phase formation and about the growth process which leads from critical nuclei to detectable crystals (Söhnel and Mullin, 1988). If the process which takes place is truly homogeneous nucleation, that is, it occurs in a clear solution under the effect of supersaturation alone, t_{ind} is inversely proportional to the nucleation rate, defined as the number of nuclei formed in solution per unit time and volume. Therefore, as shown by Mullin (1993) and Söhnel and Garside (1992), it is possible to use the experimental knowledge of the induction period to estimate two characteristic thermodynamic quantities; namely, the dependence of t_{ind} on temperature allows to evaluate the activation energy for nucleation, while its dependence on supersaturation allows to determine the interfacial tension between crystals and the surrounding solution (Söhnel, 1982; He et al., 1994). It is to be pointed out that the roles of homogeneous and heterogeneous nucleation in crystallization from solution are generally difficult to separate and then quantify. Therefore, a great attention is to be payed both from an experimental point of view by accurately preparing the feed solutions in order to exclude the presence of foreign particles, and in data treatment, by distinguishing between the two phenomena, in order to use the experimental data relative exclusively to homogeneous nucleation to estimate parameter values.

Packter (1974) studied gypsum precipitation from solutions with different calcium sulfate concentrations, and used both optical microscopy and chemical analysis; he measured induction periods, and determined crystal concentrations and dimensions. The induction period was found to decrease from 12,000 to 3 s when calcium sulfate concentration was increased from 20 to 240 mol/m^3, and the author proposed the following relationship

$$t_{ind} \propto (c - c_{eq})^{-4} \tag{1}$$

where c is calcium sulfate concentration (mol/m^3) and c_{eq} is calcium sulfate solubility (mol/m^3). However, it has to be observed that the work of Packter concerned conditions of heterogeneous nucleation, in which gypsum crystals formed on dust particles suspended in the supersaturated solution. Therefore, the results obtained could be used neither for the evaluation of the activation energy nor for that of the interfacial tension.

Sarig and Mullin (1982) investigated the effect of various additives on the induction period for gypsum crystallization. The authors used the so-called *stopped-flow* technique, which is based on the conductivity change which occurs in a supersaturated solution when nucleation takes place (Nielsen, 1964). The values of the induction periods were found to be insensitive to variations in calcium sulfate concentrations: since it is generally acknowledged that in homogeneous conditions t_{ind} is strongly dependent on supersaturation, the authors interpreted this result by suggesting that the nucleation process is heterogeneous; however, it has to be pointed out that this is at least partially in contrast with the result reported in Eq. 1 (Packter, 1974). Sarig and Mullin (1982) also investigated the effect of trace impurities, namely Al^{+3} and F^- ions, on gypsum precipitation. They found that when such ions are simultaneously present in solution, they form aluminum-fluoride complexes which retard precipitation and thus increase the induction period.

Amathieu and Boistelle (1988) studied crystallization kinetics of calcium sulfate dihydrate both in homogeneous and in heterogeneous conditions. In particular homogeneous nucleation was studied by mixing clear solutions of sodium sulfate and calcium chloride, and the induction period was measured by means of a conductimetric method described above (Sarig and Mullin, 1982). The authors showed that t_{ind} strongly depends on supersaturation (σ), decreasing from 1,200 to 60 s when σ increases from 4 to 7, and found that the following equation well describes the experimental results

$$t_{ind} \propto (\ln \sigma)^{-2} \tag{2}$$

He et al. (1994) experimentally determined induction periods for the homogeneous nucleation of gypsum in NaCl solution with NaCl concentration varying from 0 to 6 kmol/m^3 at 25°C, and in 3.0 kmol/m^3 NaCl solutions at temperatures from 25 to 90°C. They measured both Ca^{2+} concentration and turbidity, and evaluated t_{ind} as the time elapsed between the onset of supersaturation and the first observed change in any of these two variables. The authors investigated the effects of saturation level, temperature, and ionic strength on nucleation kinetics, and furthermore used the measured values of t_{ind} to determine the activation energy for gypsum nucleation and the interfacial tension between gypsum and the aqueous NaCl solution. They found that the induction period not only depends on temperature and supersaturation, but also on ionic strength, and, namely, that the higher the ionic strength, the lower t_{ind}; this last result was interpreted by assuming that, due to the nonideal behavior of concentrated ionic solutions, a correlation exists between ionic strength and gypsum solubility.

The analysis of the literature shows that few data are available for t_{ind} for gypsum nucleation in homogeneous conditions, and, therefore, for the activation energy and the interfacial tension of the crystallization process. Furthermore, most of the data have been obtained by means of chemical or photographical techniques, which are not fast and sensitive enough to give reliable measurements of relatively short induction periods (Söhnel and Mullin, 1978). With the aim of developing a more sensitive method to measure induction period for gypsum nucleation, a new technique, based on light scattering, has been devised. In this article this technique, which allows to have a continuous *in-situ* measurement of the light scattered and absorbed by the crystal suspension, is presented, and an experimental apparatus based on such a tech-

nique is described. By means of this technique, it has been possible to estimate the activation energy for gypsum crystallization and to evaluate the interfacial tension (γ_s) between $CaSO_4 \cdot 2H_2O$ and the surrounding aqueous solution.

Experimental Apparatus and Procedure

The experimental apparatus consists of a reactor with a related optical device, and is shown in Figure 1. The reactor is a batch cylindrical crystallizer, made of glass, with a working volume of 1.0×10^{-3} m^3 and a diameter of 90 mm. The crystallizer is surrounded by a water jacket for temperature control; agitation is provided by a two-blade polypropylene propeller, with agitation rate ranging between 1 and 10 s^{-1}. An off-take tube, placed at half of the working height of the vessel, allows the removal of samples from the suspension; the position of the tube has been chosen to ensure that the content of the exit stream is the same as the content of the reactor (Zacek et al., 1982).

The stream removed by the off-take tube is sent, by a peristaltic pump, to an analysis flow-through cell, and then is again conveyed to the crystallizer. The cell is made of quartz and is 70 mm long with a square section of 10 and 2.5 mm thickness. A 10-mW He–Ne laser beam ($\lambda_o = 632.8$ nm) is focused on the cell, orthogonal to its walls; the beam is vertically polarized with a diameter of 2 mm. On the path of the laser, placed at 45° with respect to beam direction, a beam splitter is provided in order to divide the laser beam into two parts; one of these is used to illuminate the measure cell, while the other one, collected by a photodiode, allows the checking of the stability and the intensity of laser beam (I_o) (W/m^2). The signal of the scattered light (I_{sca}) is collected by two focal lenses 120 and 50 mm, at 90° with respect to the laser beam; this signal is sent through a quartz optical fiber which ends on an interferential filter to a photomultiplier tube, connected to a power supply with a voltage variable in the range of 0–1,000 V. The signal of the transmitted light (I_{trans}) is collected by a photodiode located beyond the cell at 0° with respect to the laser beam. The two analog signals of scattered and transmitted light, together with I_o, are acquired and are sent to a data acquisition device (Prisciandaro, 1998).

Supersaturated solutions of calcium sulfate were prepared by mixing directly into the reactor two clear equimolar aqueous solutions of reagent grade $CaCl_2 \cdot 2H_2O$ and Na_2SO_4 in bidistilled water. After their preparation, the two solutions were filtered by using a 0.22 μm filter (Millipore) and a vacuum pump in order to eliminate all foreign material inevitably present in the solution. The concentration of each salt varied between 26 and 105 mol/m^3. The dissolved Ca^{2+} ion concentration in the solution was measured by EDTA titration using Idranal Pellets (Riedel-de Haen) as an indicator, while SO_4^{2-} ion concentration was measured by means of turbidity measurements carried out in a spectrophotometer (Hach, DREL/5).

The induction period was evaluated by measuring the intensity of both scattered and transmitted light as a function of time. Figure 2 refers to an experiment carried out at a temperature of 50°C and with initial concentrations of $CaCl_2 \cdot 2H_2O$ and Na_2SO_4 of 62.5 mol/m^3 ($\sigma = 2.73$). In the figure the ratios I_{trans}/I_o and I_{sca}/I_o are reported as a function of time, taking the moment in which the two solutions

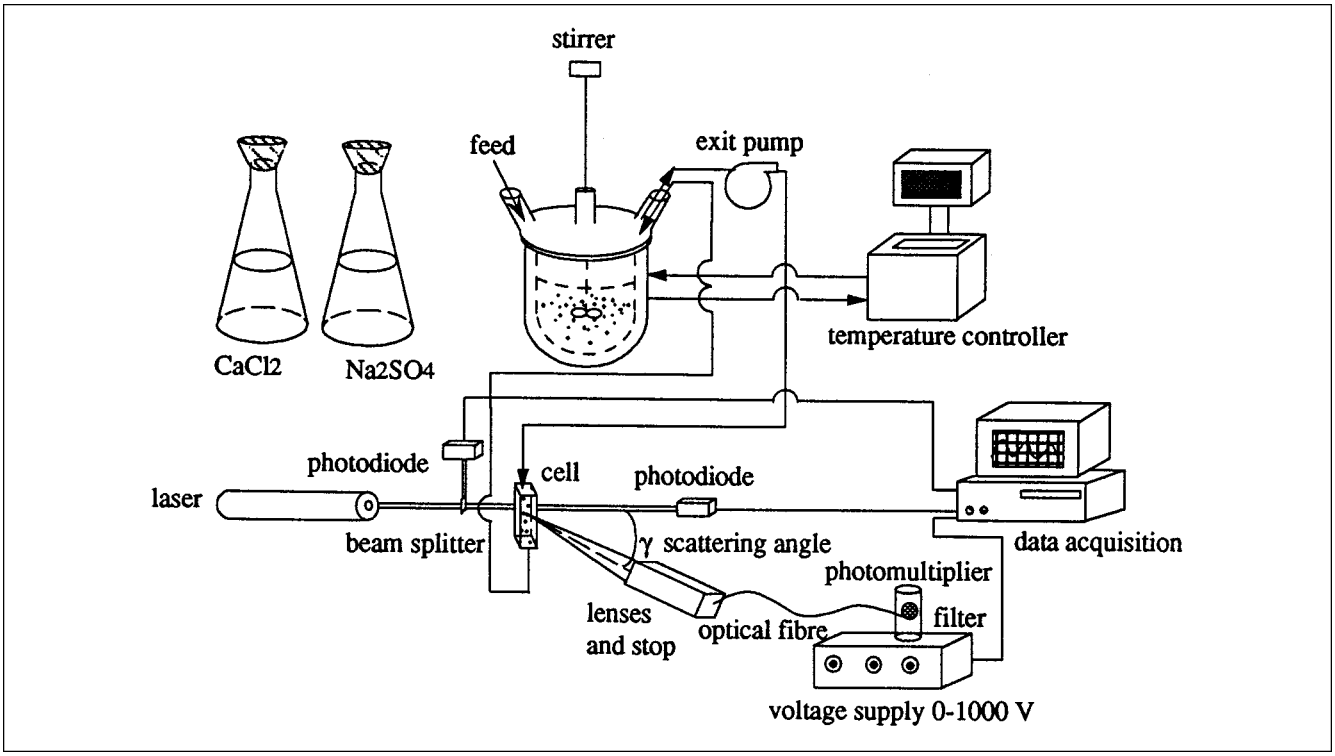

Figure 1. Experimental apparatus.

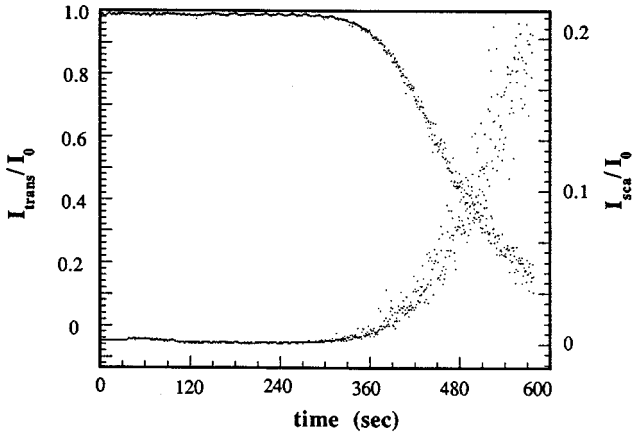

Figure 2. Intensities of the scattered (I_{sca}) and transmitted (I_{trans}) light vs. time with $\sigma = 2.73$, $T = 50°C$.

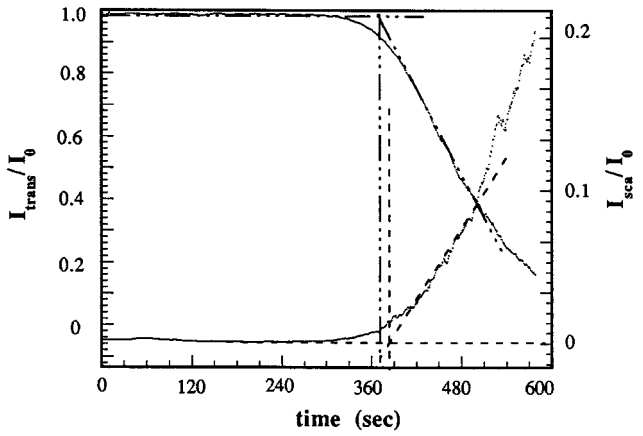

Figure 3. Intensities of the scattered (I_{sca}) and transmitted (I_{trans}) light vs. time, mobile average on 15 points with $\sigma = 2.73$, $T = 50°C$.

were brought in contact as the initial time for the experiment ($t = 0$). It can be seen that, at $t = 0$, it is $I_{trans}/I_o = 1$ and $I_{sca}/I_o = 0$, and then, as gypsum crystals start to form, I_{trans}/I_o decreases while I_{sca}/I_o increases. Both the decrease of I_{trans}/I_o and the increase of I_{sca}/I_o have an almost linear dependence on time until, at the end of the experiment, such linearity is lost. In these conditions the suspension is very dense and I_{trans}/I_o becomes close to 0, while I_{sca}/I_o reaches a *plateau* due to the onset of multiple scattering, a condition in which the measure loses its significance.

In order to find the induction period from the data of I_{sca}/I_o and I_{trans}/I_o reported in Figure 2, two parallel procedures were adopted, one graphical and the other one numerical. In the graphical procedure, the two curves were first smoothed by means of a 15-point mobile average. Afterwards, a couple of straight lines was fitted to each curve (Figure 3): for example, the I_{trans}/I_o curve was sketched by a first horizontal line ($I_{trans}/I_o = 1$), which is relative to unchanged optical properties of the solution and, therefore, to the absence of a solid phase, and by a second line which refers to the period of linear decrease with time caused by the precipitation phenomenon. The second line was drawn by positioning the best straight line on the signal corresponding to a change in slope due to the decrease of signal with respect to the initial value. A similar procedure has been symmetrically done for the curve of I_{sca}/I_o; the first horizontal line is relative to the absence of solid phase ($I_{sca}/I_o = 0$), and the second straight line was given by an increase of signal with respect to the initial value. For each curve, the intersections of the two lines gave the induction period value that in particular, for the data reported in Figure 3, it is $t_{ind} = 380$ s. In regard to the numerical method, the value of the induction period was found by making a logical test, which consists in the evaluation of the time at which the signal of scattered light (I_{sca}) was higher than 5% of its initial value I_0. (Correspondingly, the signal of transmitted light (I_{trans}) was lower than 5% of its initial value.) A significant change in the signal initial values corresponds to a modification of the optical properties detected by the laser, such as a solid phase had formed in solution. The two methods, numerical and graphical, gave results quite similar ($\pm 10\%$) and their average value was used.

Results and Discussion

In Figures 4–6 the smoothed curves of I_{sca}/I_o and I_{trans}/I_o are reported as a function of time for different supersaturation values (σ) and for three different temperatures ($T = 25$, 50, and 70°C).

The supersaturation was calculated considering the following liquid–solid equilibrium between Ca^{2+} and SO_4^{2-} ions and solid $CaSO_4 \cdot 2H_2O$

$$Ca^{2+} + SO_4^{2-} + 2H_2O = CaSO_4 \cdot 2H_2O \qquad (3)$$

so that it is

$$\sigma = \frac{a_{Ca^{2+}}\, a_{SO_4^{2-}}\, a_w^2}{K_{ps}} \qquad (4)$$

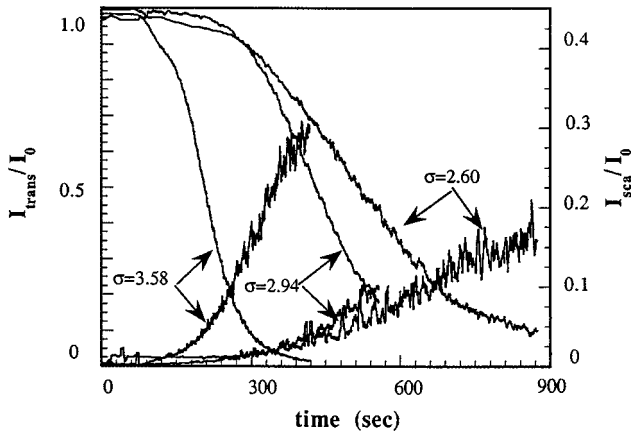

Figure 4. Intensities of the scattered (I_{sca}) and transmitted (I_{trans}) light vs. time for supersaturation values at $T = 25°C$.

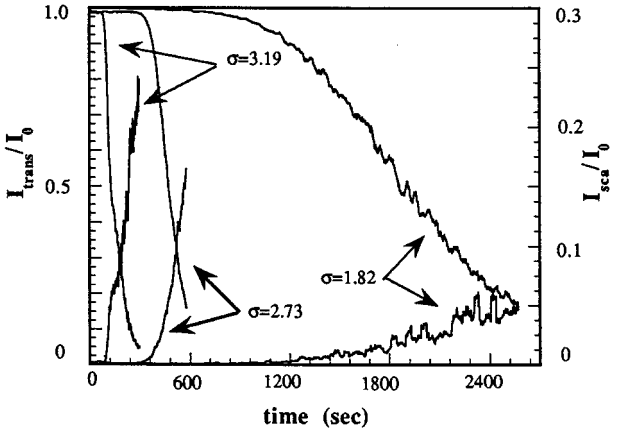

Figure 5. Intensities of the scattered (I_{sca}) and transmitted (I_{trans}) light vs. time for supersaturation values at $T = 50$°C.

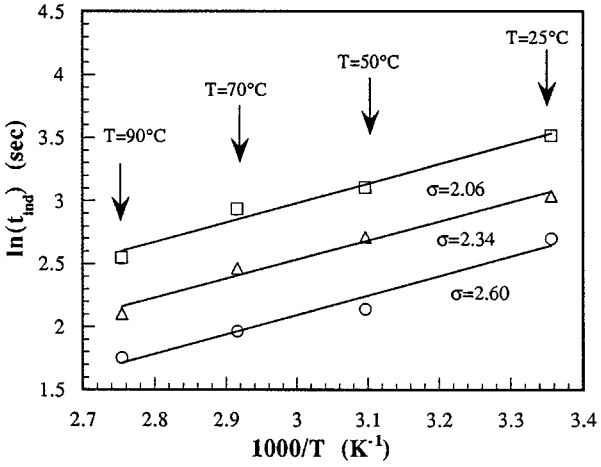

Figure 7. Dependence of the induction period on temperature: ○, σ=2.60; △, σ=2.34; □, σ=2.06.

where a_I is the activity (mol/m^3) expressed as the product of the molality (m_I) (mol/kg) and the activity coefficient (γ_I) of the I species ($I = Ca^{2+}$, SO_4^{2-} and water), and K_{ps} is the solubility product of gypsum. The value of K_{ps} (mol^4/kg^4) was calculated as a function of temperature by means of the following relationship

$$\ln(K_{ps}) = 390.9619 - 152.6246 \log T - 12{,}545.62/T + 0.0818493T \quad (5)$$

obtained by Marshall and Slusher (1966) for calcium sulfate dihydrate in aqueous sodium chloride solutions from 0 to 110°C (see also Barba et al., 1982; Budz et al., 1986). The activity coefficient calculations in the supersaturated solution are reported in the Appendix.

Figures 4–6 show that, as expected, the induction period is strongly influenced by temperature (for example, see Mullin, 1993); moreover, it can be seen that the induction period is influenced by supersaturation as well, although less strongly, and that the influence of supersaturation is stronger at low temperature than at high temperature.

In Figure 7 the logarithm of t_{ind} is reported vs. $1/T$ for three different levels of supersaturation. The analysis of the figure shows that the higher the supersaturation, the lower the induction period, and that a linear relationship does exist between the logarithm of t_{ind} and the inverse of the absolute temperature.

The dependence of the induction period on supersaturation is shown in Figure 8 for the temperatures of 25, 50 and 70°C. From this figure, it is possible to see that induction period for gypsum nucleation continuously decreases with increasing supersaturation, and that such a decrease is particularly strong at high temperature. The dependence of the induction period on supersaturation is generally described in literature by the following semiempirical correlation (Packter,

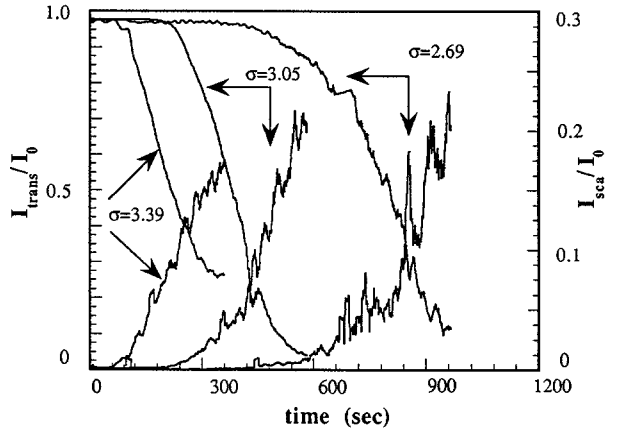

Figure 6. Intensities of the scattered (I_{sca}) and transmitted (I_{trans}) light vs. time for supersaturation values at $T = 70$°C.

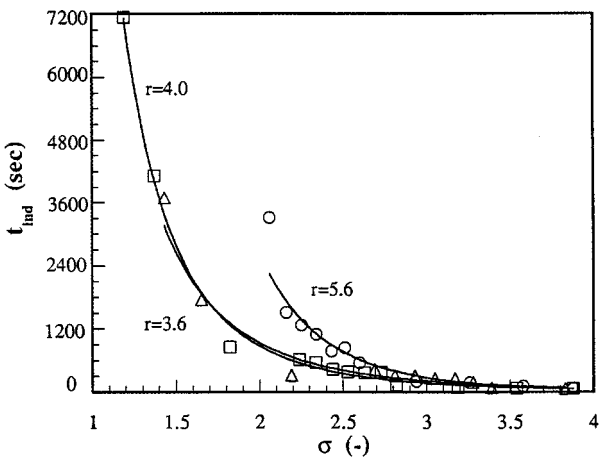

Figure 8. Induction period as a function of supersaturation: ○, $T = 25$°C; □, $T = 50$°C; △, $T = 70$°C.

1968) on which the curves correlating experimental data in Figure 8 are based on

$$t_{\text{ind}} = \frac{K}{\sigma^r} \tag{6}$$

where K (s) and r are empirical constants. In particular for $T = 25$°C, it is $K = 2{,}119$ min and $r = 5.6$; for $T = 50$°C, it is $K = 240$ min and $r = 4.0$, while for $T = 70$°C, it is $K = 193$ min and $r = 3.6$, confirming that, as previously indicated, the dependence of t_{ind} on σ is stronger at low temperature than at high temperature. Nevertheless, Eq. 6 is unable to recognize whether homogeneous or heterogeneous nucleation has occurred.

On the other side, data of t_{ind} vs. supersaturation can be used to distinguish between the two different primary nucleation mechanisms by using the correlation, derived from homogeneous nucleation equations, proposed by He et al. (1994)

$$\log(t_{\text{ind}}) = A + \frac{B}{T^3(\log \sigma)^2} \tag{7}$$

where A is an empirical constant (dimensionless) and B depends on a number of variables, and is given by

$$B = \frac{\beta \gamma_s^3 \nu^2 N_A f}{(2.3R)^3} \tag{8}$$

in which β is a shape factor, γ_s is the surface energy (J/m^2), N_A is the Avogadro number (mol^{-1}), R is the gas constant (J/mol·K), ν the molecular volume (m^3/mol), and f is a correction factor which takes into account the heterogeneous nucleation; in particular, according to Söhnel and Mullin (1988), when purely homogeneous nucleation takes place, it is $f = 1$ and when heterogeneous nucleation occurs it is $f < 1$.

Plotting $\log(t_{\text{ind}})$ against $1/[\log(\sigma)]^2$ over a sufficiently wide range of supersaturation for a fixed temperature gives a couple of straight lines with different slopes, relative to homogeneous and heterogeneous nucleation (Söhnel and Garside, 1992). As a matter of fact, the change of nucleation mechanism produces a change in the slope B; since for heterogeneous nucleation it is $f < 1$ and for homogeneous nucleation it is $f = 1$, then the value of the slope B relative to homogeneous conditions is higher than that for heterogeneous conditions. In Figure 9 this behavior is shown for $T = 50$°C: at lower supersaturation, heterogeneous nucleation is the predominant mechanism, while at higher supersaturation homogeneous nucleation is the most important phenomenon.

Taking into account values of t_{ind} relatively solely to the homogeneous nucleation region, it is possible to evaluate two thermodynamic quantities, namely, the activation energy for gypsum crystallization and the interfacial tension between gypsum crystals and the surrounding aqueous solution. The following empirical relationship, proposed by Liu and Nancollas (1975), was used to correlate data of t_{ind} vs. T

$$t_{\text{ind}} = \tau \exp\left(\frac{E_{\text{att}}}{RT}\right) \tag{9}$$

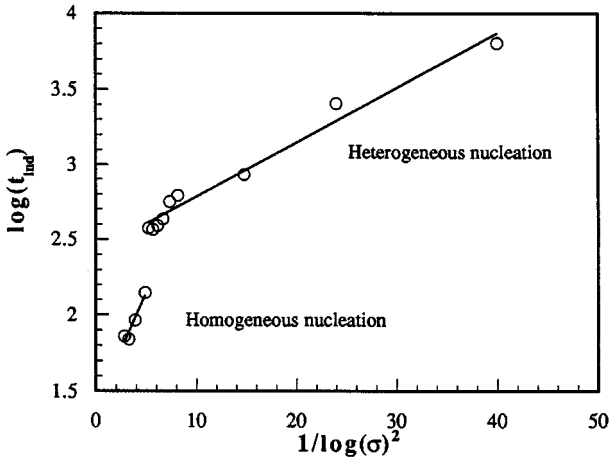

Figure 9. Induction period as a function of supersaturation (homogeneous and heterogeneous nucleation): $T = 50$°C.

where τ is a constant (s), E_{att} is the activation energy (J/mol) for the process, and R is the gas constant. In particular, Eq. 9 was reported as continuous lines in Figure 7, and from the slopes of these straight lines, the values of 30 kJ/mol was determined for the activation energy.

In Figure 9, from the slope of the straight line relative to the homogeneous nucleation ($f = 1$), it was possible to calculate the value of B, and, therefore, of the surface energy for the system gypsum–NaCl solution. Namely, in Eq. 8 it was considered $\beta = 16\pi/3$ (assuming spherical particle) and $\nu = 74.69$ cm^3/mol (He et al., 1994). The procedure described was carried out for three values of temperature ($T = 25$, 50 and 70°C), and the mean value obtained was $\gamma_s = 37$ mJ/m^2, with no significant dependence on temperature. It is useful to observe that the dependence of γ_s on T for $CaSO_4 \cdot 2H_2O$ is a controversial matter: according to some researchers, surface tension decreases with increasing temperature (Wood and Walton, 1970), while, according to others, it increases with increasing temperature either linearly (He et al., 1994) or exponentially (Rasmussen and MacKenzie, 1973).

Conclusions

Limestone slurry scrubbing is the most common commercial throwaway process for control of sulfur dioxide emissions from combustion of fossil fuels. Nucleation and crystal growth of calcium sulfate dihydrate represent an important step of this process, because they affect the scrubber solution composition, the water process balance, and the scaling problems in the absorber. A literature analysis showed that precipitation mechanisms of gypsum are not fully understood, and kinetic data are not sufficient to adequately predict gypsum nucleation kinetics. In this work an experimental apparatus consisting of a crystallizer reactor with a related optical device is presented, together with a set of experiments concerning the measurement of a gypsum induction period for nucleation as a function of temperature and of supersaturation. By using the experimental data relative to the homogeneous nucleation mechanism, the dependence of the induction period

on temperature allowed the determination of the activation energy for gypsum nucleation, while the dependence on supersaturation allowed the estimation of the interfacial tension between the gypsum and aqueous solution. The technique proposed could be applied to the evaluation of the induction period for other crystallizing systems, particularly when it is very short.

Notation

B_1 = constant in Bromley's method
V = volume, m^3
λ_o = wavelength, m

Subscripts

abs = absorption
ext = extinction
M = cation
w = water
X = anion

Literature Cited

Amathieu, L., and Boistelle, R., "Crystallization Kinetics of Gypsum from Dense Suspension of Hemihydrate in Water," *J. Cryst. Growth*, **88**, 183 (1988).

Barba, D., V. Brandani, and G. Di Giacomo, "A Thermodynamic Model of $CaSO_4$ Solubility in Multicomponent Aqueous Solutions," *Chem. Eng. J.*, **24**, 191 (1982).

Bromley, L. A., "Thermodynamic Properties of Strong Electrolytes in Aqueous Solutions," *AIChE J.*, **19**, 313 (1973).

Budz, J., A. G. Jones, and J. W. Mullin, "Effect of Selected Impurities on the Continuous Precipitation of Calcium Sulphate (Gypsum)," *J. Chem. Tech. Biotechnol.*, **36**, 153 (1986).

He, S., J. E. Oddo, and M. B. Tomson, "The Nucleation Kinetics of Calcium Sulfate Dihydrate in NaCl Solutions up to 6 m and 90°C," *J. Coll. Int. Sci.*, **162**, 297 (1994).

Liu, S. T., and G. H. Nancollas, "A Kinetic and Morphological Study of the Seeded Growth of Calcium Sulfate Dihydrate in the Presence of Additives," *J. Coll. Int. Sci.*, **52**, 593 (1975).

Marshall, W. L., and R. Slusher, "Thermodynamics of Calcium Sulfate Dihydrate in Aqueous Sodium Chloride Solutions, 0−110°," *J. Phys. Chem.*, **70**, 4015 (1966).

Mullin, J. W., *Crystallization*, 3rd ed., Butterworth-Heinemann Ltd., Oxford (1993).

Nielsen, A. E., *Kinetics of Precipitation*, Pergamon Press, Oxford (1964).

Packter, A., "Precipitation of Sparingly Soluble Alkane-Earth Metal and Lead Salts: Nucleation and Growth Orders During the Induction Period," *J. Chem. Soc.*, 859 (1968).

Packter, A., "The Precipitation of Calcium Sulphate Dihydrate from Aqueous Solution-Induction Period, Crystal Numbers and Final Size," *J. Cryst. Growth*, **21**, 191 (1974).

Prisciandaro, M., "Cristallizzazione del Solfato di Calcio Biidrato nel Processo di Desolforazione ad Umido dei Fumi Della Combustione," PhD Diss., Univ. of Naples "Federico II," Italy (1998).

Rasmussen, D. H., and A. P. MacKenzie, "Clustering in Supercooled Water," *J. Chem. Phys.*, **59**, 5003 (1973).

Ratinov, V. B., and O. M. Todes, *Dokl. Akad. Nauk SSSR*, **132**, 402 (1960).

Sarig, S., and J. W. Mullin, "Effect of Impurities on Calcium Sulphate Precipitation," *J. Chem. Tech. Biotechnol.*, **32**, 525 (1982).

Söhnel, O., "Electrolyte Crystal-Aqueous Solution Interfacial Tensions from Crystallization Data," *J. Crystal Growth*, **57**, 101 (1982).

Söhnel, O., and J. Garside, *Precipitation*, Butterworth-Heinemann Ltd., Oxford (1992).

Söhnel, O., and J. W. Mullin, "A Method for the Determination of Precipitation Induction Periods," *J. Crystal Growth*, **44**, 377 (1978).

Söhnel, O., and J. W. Mullin, "Interpretation of Crystallization Induction Periods," *J. Coll. Int. Sci.*, **123**, 43 (1988).

Wood, G. R., and A. G. Walton, "Homogeneous Nucleation Kinetics of Ice from Water," *J. Appl. Phys.*, **41**, 3027 (1970).

Zacek, S., J. Nyvlt, J. Garside, and A. W. Nienow, "A Stirred Tank for Continuous Crystallization Studies," *Chem. Eng. J.*, **23**, 111 (1982).

Appendix

The values of activity coefficients for calcium and sulfate ions as a function of ionic strength were calculated for calcium sulfate by means of the model proposed by Bromley (1973). This model gives useful correlation to estimate the mean activity coefficient of sparingly soluble electrolytes in solutions of high ionic strength. Introduction of the mean ionic activity coefficient $\gamma_{\pm}$ is necessary since the activity coefficients of individual ions cannot be independently determined; thus, an electrolyte $M_{\nu+}\,N_{\nu-}$ in solution, which dissociates to give a number ν^+ of cations and a number ν^- of anions, is thought to be composed of ions which all possess the same average properties described by the mean quantity (Söhnel and Garside, 1992)

$$\gamma_{\pm} = \left(\gamma_+^{\nu^+}\,\gamma_-^{\nu^-}\right)^{1/\nu} \tag{A1}$$

where γ_+ and γ_- are activity coefficients of individual ions, and $\nu = \nu^+ + \nu^-$.

The mean activity coefficient of the compound M_1X_1 (the subscripts "1" indicate that the salt in solution gives an equal number of cations and anions) in a multicomponent system in which a anions and c cations are present, can be determined by means of the following relationship

$$\log \gamma_{\pm} = -\frac{0.511|z_{M_1} z_{X_1}|\sqrt{FI}}{1+\sqrt{FI}} + \frac{|z_{M_1} z_{X_1}|}{|z_{M_1}|+|z_{X_1}|}\left[\frac{F_M}{|z_{M_1}|} + \frac{F_X}{|z_{X_1}|}\right] \tag{A2}$$

In this equation FI is the ionic strength (mol/m^3), which can be calculated from the following expression

$$FI = \frac{1}{2}\sum_I m_I z_I^2 \tag{A3}$$

where m_I and z_I are molality and charge of I species, respectively. F_M and F_X, on the other hand, take into account the interactions among ions in solution, and, in turn, may be evaluated by means of the following equations

$$F_M = \sum_{j=1}^{a} \overline{B}_{M_1X_j}\left(\overline{Z}_{M_1X_j}\right)^2 m_{X_j} \tag{A4}$$

$$F_X = \sum_{i=1}^{c} \overline{B}_{M_iX_1}\left(\overline{Z}_{M_iX_1}\right)^2 m_{M_i} \tag{A5}$$

with

$$\overline{Z}_{M_iX_j} = \left[|z_{M_i}| + |z_{X_j}|\right]/2 \tag{A6}$$

and

$$\overline{B}_{M_i X_j} = \frac{\left(0.06 + 0.6 B_{1, M_i X_j}\right)|z_{M_i} z_{X_j}|}{\left(1 + \dfrac{1.5I}{|z_{M_i} z_{X_j}|}\right)^2} + B_{1, M_i X_j} \quad \text{(A7)}$$

in which the subscripts i and j refer to each of the c cations and a anions present in solution, respectively.

For each compound $M_i X_j$, Bromley's model individuates a constant $B_{1, M_i X_j}$, depending on ionic contributions and defined as

$$B_{1, M_i X_j} = B_{M_i} + B_{X_j} + \delta_{M_i} \delta_{X_j} \quad \text{(A8)}$$

Table A1. Values of Ionic Contributions for Determining Constant $B_{1, M_i X_j}$

Ion	B	δ
H^+	0.0875	0.103
Ca^{2+}	0.0374	0.119
Na^+	0	0.028
OH^-	0.076	−1.0
SO_4^{2-}	0	−0.40
Cl^-	0.0643	−0.067

where the values of B and δ have been estimated for different cations and anions, and for the ions of the system $CaSO_4 \cdot 2H_2O$ in NaCl solution are reported in Table A1.

Manuscript received Apr. 21, 1998, and revision received Oct. 27, 1998.